Pergamon

0045-7949(94)00513-3

Computers & Structures Vol. 55, No. 6, pp. 1015–1025, 1995

0045-7949/95 $9.50 + 0.00

THE SOFT WAY METHOD AND THE VELOCITY FORMULATION

C. Bajer† and **C. Bohatier**‡

†Institute of Fundamental Technological Research, Polish Academy of Sciences, Świętokrzyska 21, 00-049 Warsaw, Poland

‡French Institute of Advanced Mechanical Engineering, B.P. 265, 63175 Aubière, France

(*Received* 10 *December* 1993)

Abstract—In this paper the new approach to dynamic contact problems is described. The velocity formulation was assumed and a new time integration scheme was elaborated. The space–time finite element method used in derivation enables control of the accuracy (order of the error) and stability. Methods for the solution of contact problems were discussed. A discretized approach, prepared for large displacements and large rotations, enabled real engineering problems to be solved in a relatively short time.

1. INTRODUCTION

Classical approaches to time integration of differential equations of motion for dynamic or quasi-dynamic problems are composed of two stages. First, after the choice of the formulation, the discretization of spatial domain is carried out. Then the resulting numerical procedure is applied to integrate time derivatives. More precisely, the system of partial differential equations is replaced by the system of ordinary differential equations with respect to time and then another, strictly numerical method enables the sequence of algebraic equations systems to be obtained. Such an approach has some advantages: in both stages the most efficient numerical tools can be chosen, including analytical methods. Moreover, the path from statics to dynamics is simple, since most of the procedures applied are still valid. The solution of the dynamic problem is reduced to the solution of a sequence of static problems. We have here a great number of contributions to the estimation of error, stability analysis, efficiency, etc.

However, one disadvantage is the necessity of application of stationary partition of the domain considered. The second limitation concerns the necessity of application of the same numerical procedure to all joints of the discrete mesh. Unconditionally stable procedures allow the efficiency of calculation to be increased but at the same time introduce the amplitude and phase error, which is different in different zones of the structure. Mesh refinement can improve the precision, but on the other hand it can worsen the effect of time integration. Local interference into the method of integration in time, on the level of finite element or material data data is, generally, impossible.

It is clear that the evaluation of solution methods is difficult and complex. The choice of the numerical tool depends on the problem to be solved, the type of phenomenon which has to be investigated, the precision required, the computer being used and other factors.

Different kinds of description can be used for a large deformation description. A material description is necessary to take into account the solid deformation. The more secure one for mechanical engineers is the total Lagrangian description, where the reference configuration is the initial configuration. Difficulties come from the numerous transport operations that have to be carried out during the evolution of the deformation process. Furthermore, when the boundary conditions change it complicates their relation to the initial boundary.

The last remark requires the mechanical engineer to update the configurate at each time step, then the reference configuration becomes the configuration at the beginning of the time step t_0. However, the problem of tensor transport does not disappear. Therefore another type of description seems to be more suitable. The first requirement is to have no transport term. This is the case of small perturbation theory where the configuration at the beginning of time step t_0 is the reference configuration. This kind of description is a step-by-step description, but if the time step is not sufficiently short, the accuracy of results is not certain. That is why we proposed in Ref. [1] the estimation of the configuration at the end of time step t_1. When the approximation is calculated from the velocity field at t_0 we have the explicit method. When the approximation requires the unknown velocity field at t_1, the method is implicit. The space–time finite element method improves this kind of description because of the continuity of the domain estimation. It results in the possibility of the choice of any configuration as the reference

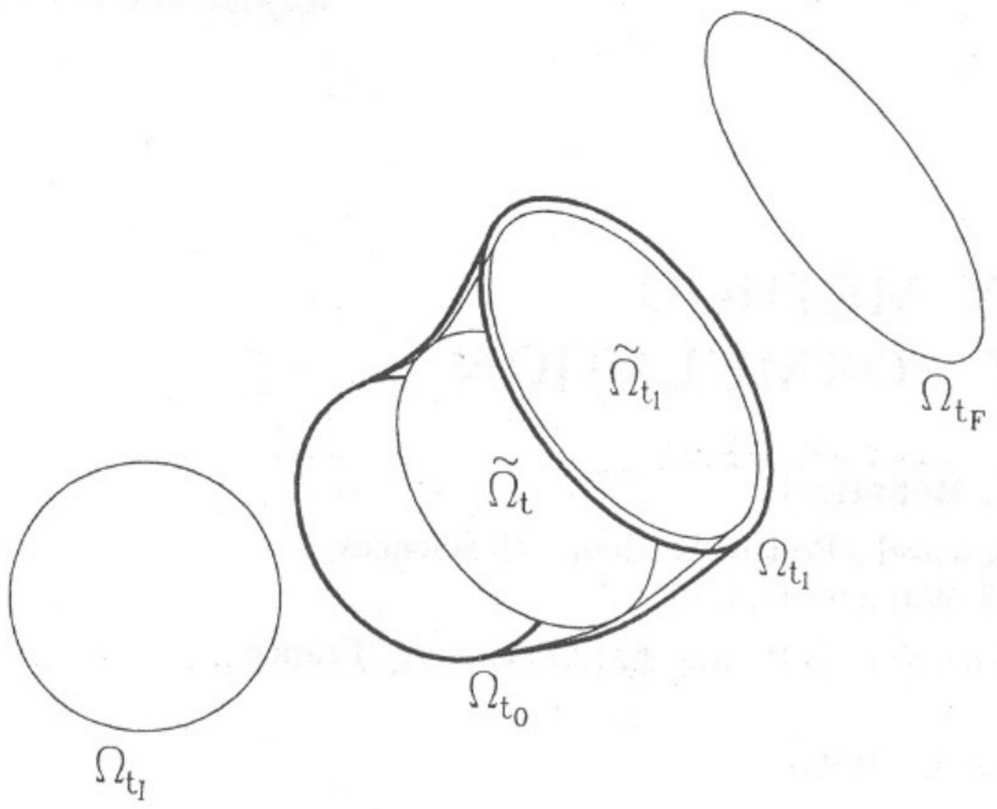

Fig. 1. Description of the evolution of the domain deformation.

configuration within the time step. If we have a linear interpolation for displacements, the domain at t can be simply described by the formula (the Minkowski transformation) (Fig. 1):

$$\Omega_t = \Omega_{t_0}\left(1 - \frac{t - t_0}{h}\right) + \Omega_{t_1}\frac{t - t_0}{h}, \quad h = t_1 - t_0. \quad (1)$$

If we have a linear interpolation for the velocity, Ω_t depends on $\mathbf{x}_0$, $\mathbf{v}_0$, $\mathbf{v}_1$:

$$\mathbf{x} = \mathbf{x}_0 + \mathbf{v}_0\frac{1}{2}(2 - \tau)h + \mathbf{v}_1\frac{\tau}{2}h, \quad (2)$$

where

$$\tau = \frac{t - t_0}{h}, \quad h = t_1 - t_0, \quad \Omega_{t_0} = \{\mathbf{x}_0\},$$

$$\Omega_{t_1} = \{\mathbf{x}_0\} + \left\{\frac{\mathbf{v}_0 + \mathbf{v}_1}{2}h\right\}.$$

The solution of the velocity field will be searched as a product of a space function and a time function.

On this short background we can place the space–time approximation. Essentially, the basic principle of the method concerns the way of approximation. Characteristic functions (i.e. displacements, velocities) are described in space–time sub-domains by nodal parameters:

$$\mathbf{u}(\mathbf{x}, t) = \mathbf{N}(\mathbf{x}, t)\mathbf{q}_e, \quad (3)$$

where $\mathbf{N}(\mathbf{x}, t)$ is the matrix of interpolation functions, which depends on spatial and time variables. Such an approach assumes the continuous distribution of characteristic quantities in the whole space–time domain Ω, in which the structure is considered $\Omega = \{\mathbf{x}, t : \mathbf{x} \in V(t), 0 \leqslant t < \infty\}$. In discrete time t_i, $i = 1, 2, \ldots$, we can use different bases of nodes (limited by certain restrictions) and, according to this feature, we can adjust the mesh to our current requirements. The following facilities can be gained:

- mesh redistribution according to the error distribution, which varies in time;
- relocation of the condensed mesh together with moving load;
- the use of different forms of meshes (different from the multiplex type, which is a result of evolution of the spatial mesh in the time layer); some meshes have certain interesting properties;
- simple individual formulation of properties of time integration, separately for each finite element;
- in a particular case the space–time approximation can be reduced to the classical solution method, based on the evolution of the material mesh.

The last point can be developed to the statement, that the space–time approximation and the method of the space–time finite elements can be considered as a generalization of the finite element method (which in fact is directly applied only to spatial domain).

The first attempt at real space–time discretization was done by Oden [2]. He proposed a general approach to the finite element method and extended the imaging of the structure on time variables. Unfortunately, this interesting idea of the non-stationary partition of the structure on subspaces was not continued. In some papers [3–6] the authors formulated problems with space and time treated equally. However, in the final stage the discretization was carried out separately for time and space (for example, Ref. [7]). Independently of the researchers mentioned above, Kaczkowski in his papers [8, 9] introduced for the first time some abstract physical terms to mechanics: the equation of time work, mass as a vector quantity or a space–time rigidity. The synthesis of the new approach can be found in Ref. [10] and stability considerations in Refs [11, 12]. In the last publication the authors described space–time elements, which lead to unconditionally stable solution schemes. Unfortunately, they could be applied only for the space–time forms, which are rectangular in time, obtained as a vector product of spatial doman and time interval. In the following works research turned to non-rectangular shapes [13, 14] and applied the approaches to different problems [15–18]. The state of the art in the space–time finite element method can be found in Refs [19–21].

2. VELOCITY FORMULATION

One degree of freedom system

Let us consider free vibration of a simple oscillator

$$m\frac{\mathrm{d}v}{\mathrm{d}t} + kx = 0. \quad (4)$$

The virtual power principle applied to eqn (4) gives the following equation:

$$\left(m\frac{\mathrm{d}v}{\mathrm{d}t}+kx\right)v^*=0 \quad \text{or} \quad w^*=0. \tag{5}$$

The principle of virtual work can be written then

$$\int_0^t \mathscr{P}^*\,\mathrm{d}t = w^* = 0. \tag{6}$$

Real velocity is linearly distributed in the time interval $(0 \leqslant t \leqslant h)$

$$v=\left(1-\frac{t}{h}\right)v_0+\frac{t}{h}v_1. \tag{7}$$

The displacement $x(t)$ is described by the integral

$$x(t)=x_0+\int_0^t v\,\mathrm{d}t. \tag{8}$$

As a virtual velocity we can assume several functions. Here we choose a function that tends to the Dirac distribution, which depends on the parameter α $(0 \leqslant \alpha \leqslant 1)$ and only on the velocity v_1:

$$v^*=\lambda v_1\,\delta\left(\frac{t}{h}-\alpha\right). \tag{9}$$

λ is a constant which normalizes the distribution v^*: $\lambda v_1 = 1$. The choice of the Heaviside function H for description of the velocity v^*,

$$v^*=\lambda v_1 H\left(\frac{t}{h}-\alpha\right), \tag{10}$$

gives the momentum equation.

Equation (4) is multiplied by v^*, with respect to eqns (7) and (8). The equation of virtual work obtained is now integrated over the time interval. Simple calculation results in the following formulae:

$$v_1=\frac{1-\dfrac{kh^2}{2m}[1-(1-\alpha)^2]}{1+\dfrac{k\alpha^2h^2}{2m}}v_0-\frac{k}{m}\frac{h}{\left(1+\dfrac{k\alpha^2h^2}{2m}\right)}x_0. \tag{11}$$

Displacement x_1 in a successive moment is determined from the velocity v_0 and v_1:

$$x_1=x_0+h[(1-\beta)v_0+\beta v_1]. \tag{12}$$

One can verify that the energy is preserved for $\beta = 1-\alpha$. With respect to this we can write the stepping scheme

$$\begin{Bmatrix} v_1 \\ x_1 \end{Bmatrix} = \begin{bmatrix} 1-\dfrac{2\alpha\kappa}{2+\alpha^2\kappa} & -\dfrac{2\kappa}{h(\alpha^2\kappa+2)} \\ 3h-\dfrac{2h(\alpha\kappa+2)}{\alpha^2\kappa+2} & \dfrac{2\kappa(\alpha-1)}{\alpha^2\kappa+2}+1 \end{bmatrix} \begin{Bmatrix} v_0 \\ x_0 \end{Bmatrix} \tag{13}$$

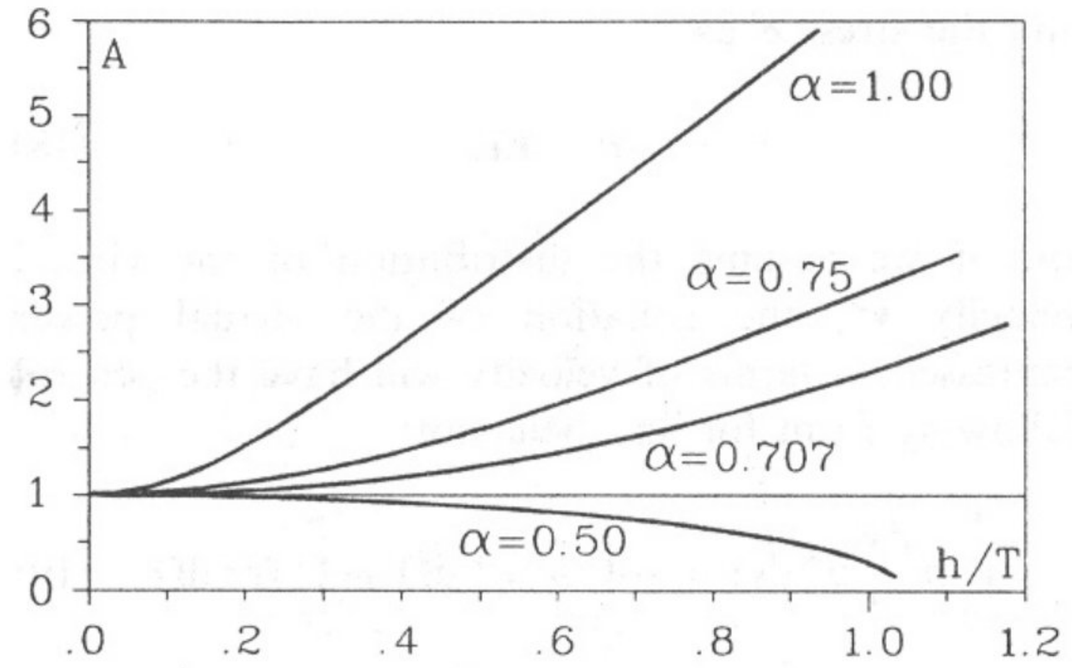

Fig. 2. The displacement amplitude for selected parameters α.

where $\kappa = h^2k/m$. The 2×2 transfer matrix $\mathbf{T}$ defined in eqn (13) allows the stabilty condition for $h\to\infty$ to be found. Eigenvalues of $\mathbf{T}$ are:

$$\lim_{h\to\infty}\lambda_{1/2}=\frac{\alpha^2-1}{\alpha^2}\pm\frac{i\sqrt{2\alpha^2-1}}{\alpha^2} \tag{14}$$

and their modules are

$$\lim_{h\to\infty}|\lambda_{1/2}|=\begin{cases}1, & \text{if } \sqrt{2}/2 \leqslant \alpha \leqslant 1\\ \dfrac{1}{\alpha^2}\sqrt{\alpha^4-4\alpha^2+2}, & \text{if } 0 \leqslant \alpha < \sqrt{2}/2.\end{cases} \tag{15}$$

We can notice that for $\alpha = 1/2$

$$x_1=x_0+\int_{t_0}^{t_1} v\,\mathrm{d}t, \tag{16}$$

where v is defined by eqn (7). Both the modules are equal to one when $\alpha \geqslant \sqrt{2}/2$. This important inequality allows us to assume for calculations the unconditionally stable procedure.

The amplitude of the velocity is almost exact. In turn the error of the displacement amplitude arises from the phase error. It is the elongation of the period of vibration, which appears when a large time step h is applied. In such a case the system is more elastic and it responds to increase in the displacement amplitude. The error of displacement amplitude for selected values of time step related to the period of vibrations T is depicted in Fig. 2. We should emphasize that the formulation by the virtual work theorem does not lead to the Galerkin method for the space–time interpolation formulation.

General case of linear elasticity (small rotations)

For the arbitrary problem of elasticity we can apply the same procedure as in the case of the one-degree-of-freedom system.

If we denote the strain ϵ as

$$\epsilon = \tfrac{1}{2}(\mathrm{grad}\,\mathbf{u}+\mathrm{grad}^{\mathrm{T}}\,\mathbf{u}) \tag{17}$$

and the stress $\boldsymbol{\sigma}$ as

$$\boldsymbol{\sigma} = \mathbf{E}\epsilon, \tag{18}$$

and if we assume the distribution of the virtual velocity $\mathbf{v}^*$, the equation of the virtual power expressed in terms of velocity will have the general following form for any behavior:

$$\int_\Omega \rho \frac{\partial \mathbf{v}}{\partial t} \mathbf{v}^* \, \mathrm{d}\Omega = -\int_\Omega \boldsymbol{\sigma} : \dot{\epsilon}^* \, \mathrm{d}\Omega + \int_\Omega \mathbf{f}\mathbf{v}^* \, \mathrm{d}\Omega, \tag{19}$$

where $\mathbf{f}$ contains all the volume forces. Displacement $\mathbf{u}(t)$ is described by the integral

$$\mathbf{u}(t) = \mathbf{u}_0 + \int_0^t \mathbf{v} \, \mathrm{d}t. \tag{20}$$

With respect to eqns (17), (18) and (20) we can develop the form of eqn (19):

$$\int_\Omega (\mathbf{v}^*)^{\mathrm{T}} \rho \frac{\partial \mathbf{v}}{\partial t} \, \mathrm{d}\Omega + \int_\Omega (\mathscr{D}\mathbf{v}^*)^{\mathrm{T}} \mathbf{E} \underbrace{\mathscr{D}\mathbf{u}_0}_{\epsilon_0} \, \mathrm{d}\Omega + \int_\Omega \left[(\mathscr{D}\mathbf{v}^*)^{\mathrm{T}} \mathbf{E} \mathscr{D} \int_0^t \mathbf{v} \, \mathrm{d}t \right] \mathrm{d}\Omega = \int_\Omega (\mathbf{v}^*)^{\mathrm{T}} \mathbf{f} \, \mathrm{d}\Omega. \tag{21}$$

Here $\mathscr{D}$ is a differential operator (whose form depends on the type of the structure) with respect to spatial coordinates and $\mathbf{f}$ is the external load.

3. UNILATERAL CONTACT AND FRICTION

The unilateral contact conditions can be enforced by numerous methods [22]. We can classify them into three groups.

Category 1: *geometrical constraint methods* [1]

- The explicit projection method is easy to carry out, but mass conservation is not satisfied during the deformation process. The contact forces are not directly known. Figure 3 shows the elementary example where the loose mass is visualized after projection onto the contact surface of points that penetrate.
- The implicit projection method leads to a good control of mass conservation. The contact forces are not directly known, but it is possible to value their reduction by the contribution of their distributions. It is necessary to control the sign of the normal forces to allow the contact point the possibility to leave or keep the contact. This method can be improved by the introduction of modified unilateral constraints restriction of the geometrical motion (geometrical soft way method) and then have some similarity to the penalty method on this displacement for velocity formulation (dual soft way method).

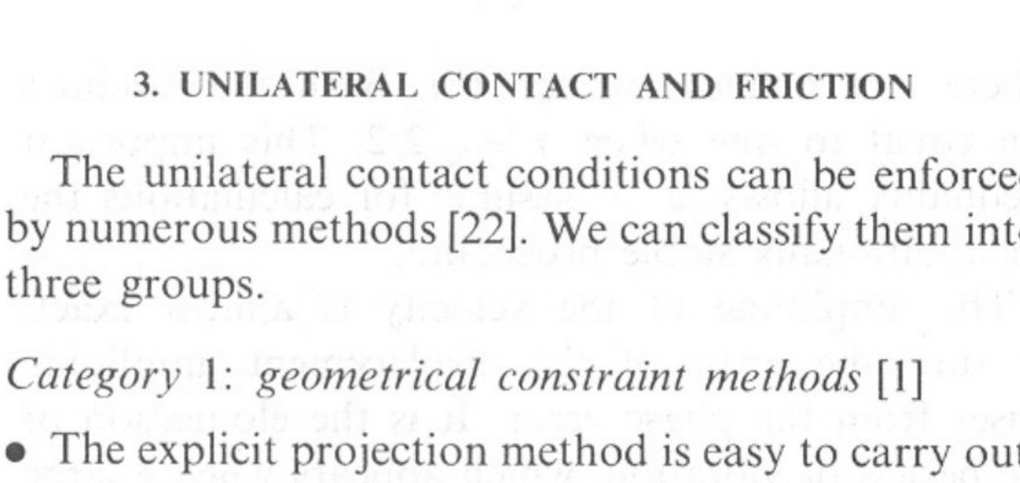

Fig. 3. The explicit projection method.

Category 2: *penalty methods*

- Penalty on normal displacement constraints with the displacement formulations [23]: this kind of method is adapted for incremental description and for small increments of deformation.
- Penalty on normal velocity constraints with velocity formulation: this method is limited to the point that keeps contact because of the numerical instability in the case of variation of the contact status.
- Penalty on normal displacement constraints with velocity formulation: the normal displacement is only significant for the contact status, the normal displacement is calculated by the integration of the velocity. We call this method the dual soft way method because of the physical analogy of the possibility of a little penetration associated with a proportional normal force directed in the opposite direction. This method is well adapted when the contact term does not become the preponderant term.

Category 3: *mixed methods* [24, 27, 25]

- The Lagrangian methods lead to an increased equation system which is more ill conditioned. Most of time the convergence is poor. For this reason the augmented Lagrangian methods improve the numerical convergence.
- The augmented Lagrangian method with Usawa's algorithm leads to an iterative process of the solution with two separate problems: velocity problem classically dimensioned, and a contact force problem with the velocity as a parameter.
- The formulation as a complementary problem with variational inequality is used in Ref. [26]. It is very efficient for the systems of rigid solids. In Ref. [27] it has been applied in deformable solid problems.

Our choice here is either the implicit projection method or the soft way method.

3.1. *Unilateral contact conditions—different modeling methods*

We introduce here the motion of reference solid. $\delta\mathbf{x}$ is the displacement $\mathbf{P}_0\mathbf{P}_1$ (Fig. 4):

$$\delta\mathbf{x} = \int_{t_0}^{t_1} \mathbf{v} \, \mathrm{d}t \tag{22}$$

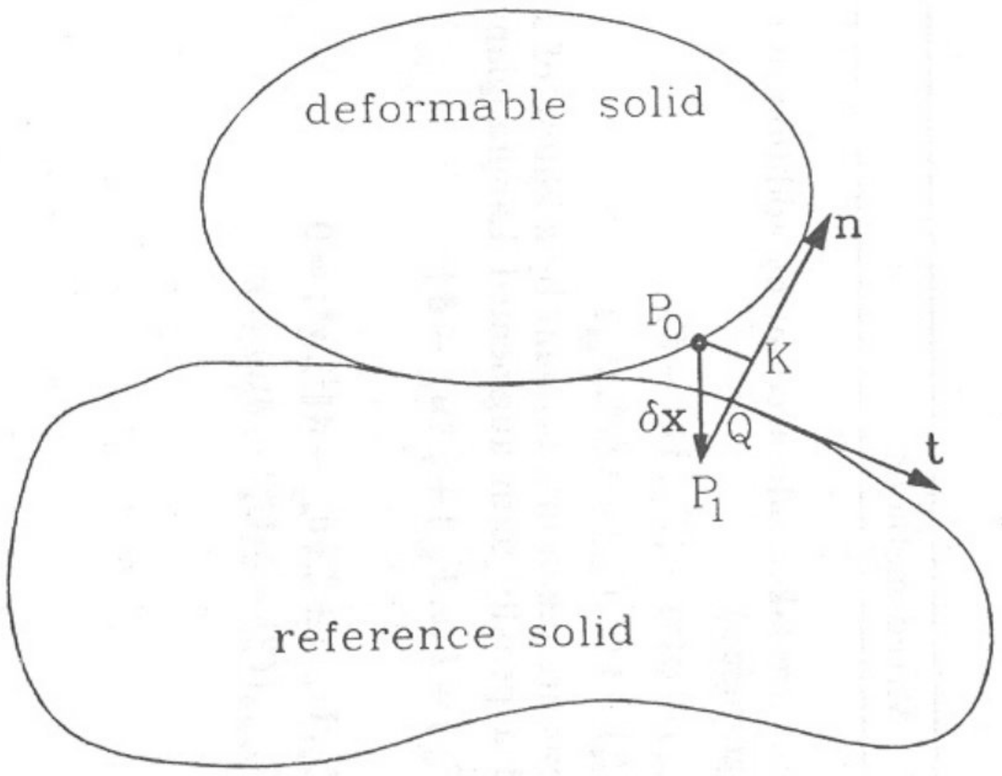

Fig. 4. Configuration before the starting of deformation process and evolution of the point P.

and

$$\mathbf{u}_n = \delta \mathbf{x} \cdot \mathbf{n} - d. \tag{23}$$

The gap **d** denoted QK in the Fig. 4 is calculated by:

$$d = (\mathbf{P}_1\mathbf{P}_0 - \mathbf{P}_1\mathbf{Q}) \cdot \mathbf{n}. \tag{24}$$

F is the contact force, compounded by a normal force related to the unilateral contact and a tangential force related to the friction phenomena.

$$\mathbf{F} = \mathbf{F}_n + \mathbf{F}_t, \tag{25}$$

where $F_n = \mathbf{F} \cdot \mathbf{n}$ is the normal force, $\mathbf{F}_n = F_n \cdot \mathbf{n}$, $\mathbf{F}_t = \mathbf{F} - \mathbf{F}_n$ is the tangential force.

The general and systematic notation for the junction between any solids in the system is presented in Fig. 5.

In most real problems, at least a couple (sometimes more) of solids are deformable. They have not necessarily the same behavior.

Consequently, it is necessary to establish more accurate notations in order to ensure a good modeling of interactions between the solids. It is very important to notice that the contact conditions are formulated by the normal displacements. When the velocity formulation is used, the formulation of the contact conditions (non-penetration conditions) is correct if $\delta \mathbf{x}$ is calculated by the expression (22). The unilateral contact conditions or Signorini conditions are

$$u_{n_{ji}} \leqslant 0$$

$$F_{n_{ij}} \leqslant 0$$

$$F_{n_{ji}} \cdot u_{n_{ij}} = 0, \tag{26}$$

where the quantities are valued on the external normal of the solid j; $\mathbf{u}_{n_{ji}} = u_{n_{ji}} \cdot \mathbf{n}_{ij}$ is the relative displacement of the solid j with regard to the solid i

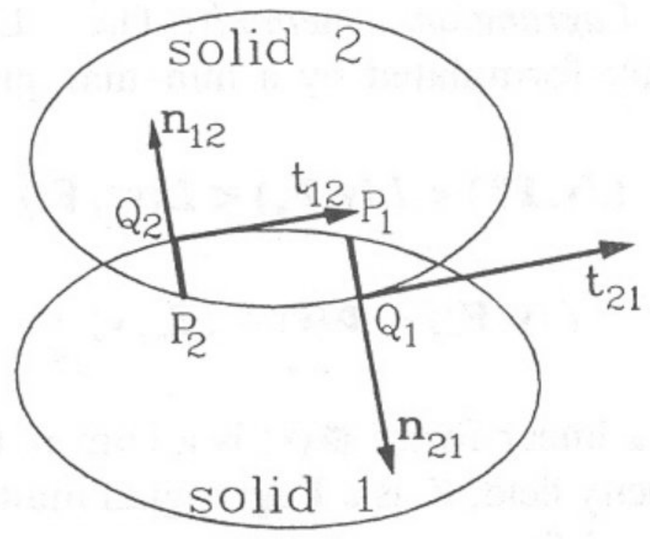

Fig. 5. Interaction modeling at an estimation for the estimated configuration within the time step of the deformation process.

and $\mathbf{F}_{n_{ij}} = \mathbf{F}_{n_{ij}} \cdot \mathbf{n}_{ji}$ is the interaction of the solid i onto the solid j (Fig. 5). At this stage it is possible to choose a method to solve the complementary problem.

3.1.1. *The projection methods.* Explicit projection: during a time step the free boundary keeps the same status. At the end of the time step, the point P_1 that came through the boundary of the solid S_2 is projected onto the solid S_2 at Q_1 and then it keeps the contact status. The normal velocity is set equal to zero and the tangential velocity is unchanged. The sign of the nodal force can be controlled. It is necessary to take small time step in order to keep good accuracy during the deformation process.

Implicit projection: during a time step the same status of contact points and free boundary points is controlled. The point P_1 that came through the boundary of the solid S_2 at the estimated configuration is projected onto the solid S_2 at a point inside the segment P_1Q_1, related to the dynamic conditions of the solids S_1 and S_2 estimated at time t_0, and then it keeps the contact status. The normal velocity at the end of the time step is settled equal to zero and the tangential velocity is free to change, then a new approximation of the configuration at the end of the deformation process can be calculated. At each contact point a control of the sign of the normal force is made in order to determine the status *free point* or *contact point*. The time step can be chosen to be much larger during the deformation process than in the explicit method.

3.1.2. *The penalty methods.* According to our choice of the velocity formulation the penalty methods of the normal displacement constraints lead to the formulation of the normal force:

$$\mathbf{F}_{n_{ij}} = \zeta \mathbf{u}_{n_{ji}} H(-u_{n_{ji}}), \tag{27}$$

where $H(\cdot)$ is the Heaviside distribution. $\zeta = 1/\epsilon$ with a small ϵ. The particularity of this method that we call the soft way method is to take the velocity as a main variable. The numerical method that can be forward selected is particularly well adapted to this modelling.

3.1.3. *Lagrangian methods.* The Lagrangian methods are formulated by a min–max problem:

$$L(\mathbf{v}, \mathbf{F}_n^*) < L(\mathbf{v}, \mathbf{F}_n) < L(\mathbf{v}^*, \mathbf{F}_n) \tag{28}$$

where

$$L(\mathbf{v}, \mathbf{F}_n) = \boldsymbol{\Phi}(\mathbf{v}) + \langle \mathbf{F}_n, \mathbf{v} \rangle. \tag{29}$$

$\langle \mathbf{F}_n, \mathbf{v} \rangle$ is a linear form, $\boldsymbol{\Phi}(\mathbf{v})$ is a convex functional of the velocity field, $\mathbf{F}_n$ is a Lagrangian multiplier that is the normal force.

The augmented Lagrangian is described by the formula

$$L_\zeta(v, F_n) = L(v, F_n) + \frac{\zeta}{2} \| u_n - d \|^2. \tag{30}$$

The Usawa algorithm [17] leads to an easy alternative solution of the mixed problem: an estimation of the normal forces gives a new velocity field. Then a new approximation of the normal force can be calculated. The paper [24] proposes a good way using the generalized Newton–Raphson method.

Table 1 is the abstract of methods for the unilateral contact with the velocity formulation.

The notation $(D\varphi, \mathbf{v}^*)$ defines the Gâteaux derivative of φ to the direction $\mathbf{v}^*$.

3.2. *Friction law*

The friction conditions can be defined as a dissipation condition:

$$\mathbf{F}_t \cdot \mathbf{v}_t \leqslant 0. \tag{31}$$

The friction law can be established with the formulation:

$$\mathbf{F}_t = \mathscr{H}(\mathbf{v}), \tag{32}$$

where $\mathscr{H}(\mathbf{v})$ is a history functional of the velocity that satisfies the same principles as the rheological law. The friction law is chosen as the surface formulation respectively either the considered solid behavior or the intermediate continuum media. Examples of friction law:

- Coulomb law (see Ref. [28, Fig. 6])—when $|F_t| < f\,|(u_n/\epsilon)H(u_n)|$ then $v_t = 0$ and $F_t = \mathscr{H}(u_n, v_t) = -f\,|(u_n/\epsilon)H(u_n)|\,\mathrm{sgn}(v_t)$.
- Viscoplastic friction law (Fig. 7):

$$\mathbf{F}_t = -\alpha\,|v_t|^{p-1} v_t \tag{33}$$

or regularized

$$\mathbf{F}_t = -\alpha\,|v_t + v_0|^{p-1} v_t. \tag{34}$$

It should be emphasized that a friction law can be established as a surface behavior law that can

Table 1. Review of the modeling methods for unilateral contact problems

Projection methods	Penalty methods	Mixed methods
Explicit $(D\varphi(\mathbf{v}), \mathbf{v}^*) = 0$ Boundary conditions: for each point coming into contact when $F_{nij}(\mathbf{v}(t_0), t_1) < 0$ is satisfied $\mathbf{u}_{n_{ij}} - h = 0,\ \forall\, t \in [t_0, t_1]$ $\mathbf{v}_{n_{ij}} = 0,\ \forall t \in [t_0, t_1]$ $\mathbf{v}_{T_{ij}} = \mathbf{v}(t_0) \cdot \mathbf{n}_{ij},\ \forall t \in [t_0, t_1].$ When $F_{nij}(\mathbf{v}(t_0), t_1) \geqslant 0$ in a point, then this point becomes a free surface point. $(D\varphi(\mathbf{v}), \mathbf{v}^*) = 0$ *Implicit* For each point coming into a contact when $F^{(k)} < 0$ is satisfied: $\mathbf{u}_{n_{ij}}^{(k)} - \mathbf{d} = 0$ $\mathbf{v}_{n_{ij}}^{(k)}(t) = 0$ $\mathbf{v}_{T_{ij}}^{(k)}(t) = \mathbf{v}_{ij}^{(k)}(t) \cdot \mathbf{n}_{ij}.$ When $F_{n_{ij}}^{(k)} \geqslant 0$ in a point, then this point becomes a free surface point. For the next iteration (k) is the estimation at the approximated configuration k.	The boundary conditions are taken into account by the addition of a penalty term: $(D(\varphi(\mathbf{v}) + \zeta \,\|\, \mathbf{u}_{n_{ij}} - \mathbf{d} \,\|^2), \mathbf{v}^*) = 0$ with $\mathbf{u}_{n_{ij}}(t) = ((\int_{[t_0, t]} \mathbf{v}\, dt)\mathbf{n}_{ji}(t))\mathbf{n}_{ji}(t).$	The boundary conditions are taken into account by addition of a multiplicand term (Lagrangian) $L(v, F_{n_{ji}}) - \varphi(\mathbf{v}) + \langle F_{n_{ji}}, \mathbf{U}_{n_{ij}} - \mathbf{d} \rangle$ $L(v, F_{\mathrm{nji}}^*) \leqslant \mathrm{L}(\mathrm{v}, \mathrm{F}_{\mathrm{nji}}) \leqslant \mathrm{L}(\mathrm{v}^*, \mathrm{F}_{\mathrm{nji}}).$ The boundary conditions are taken into account by addition of a multiplicand term and a penalty term augmented Langrangian: $L_\zeta(v, F_{n_{ij}}) = L(v, F_{n_{ij}}) + \zeta \,\|\, \mathbf{u}_{n_{ij}} - \mathbf{d} \,\|^2$ Usawa algorithm: $(D(\varphi(\mathbf{v}) + \langle F_{n_{ji}}, \mathbf{U}_{n_{ij}} \rangle + \zeta \,\|\, \mathbf{u}_{n_{ij}} - \mathbf{d} \,\|^2), \mathbf{v}^*) = 0$ $\mathbf{F}_{n_{ji}}^{k+1} = \mathrm{proj}_{F_n \geqslant 0}(\mathbf{F}_{n_{ji}}^{(k)} - \zeta(\mathbf{U}_{n_{ij}}^{(k)} - \mathbf{d}))\mathbf{n}_{ji}(t).$

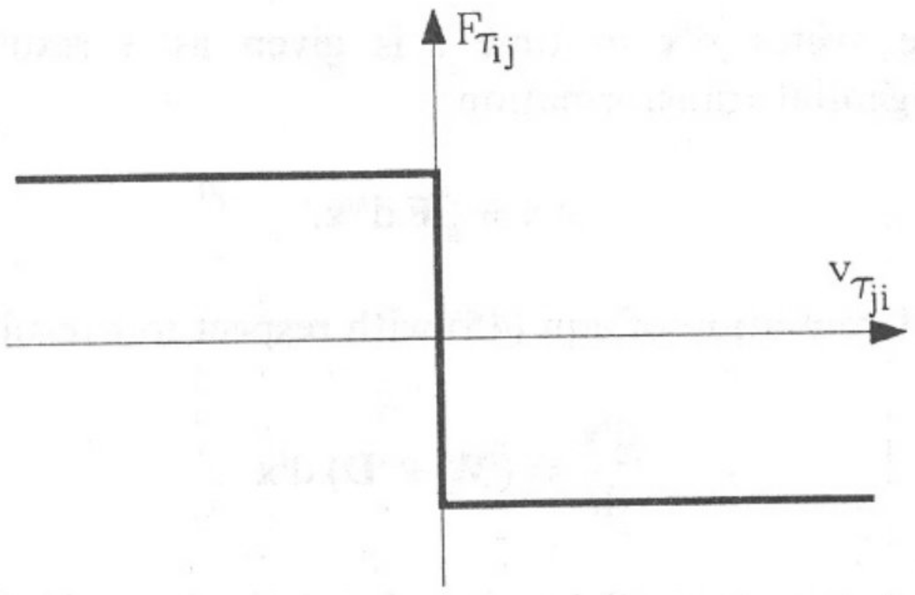

Fig. 6. Graph (v_τ, F_τ) of the Coulomb friction law.

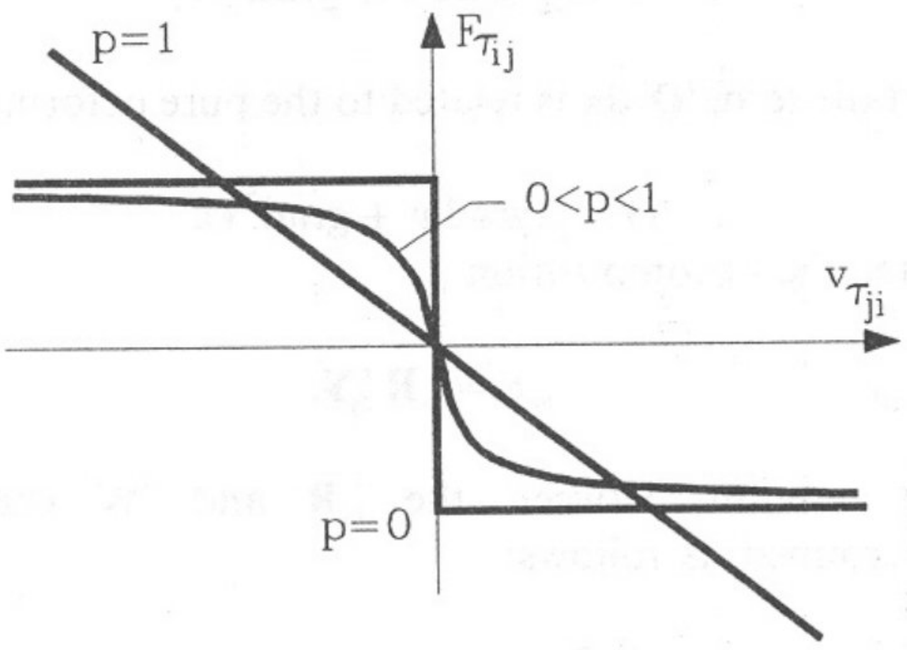

Fig. 7. Graph (v_τ, F_τ) of the viscoplastic friction: $F_{\tau ij} = -\alpha |v_{rji}|^{p-1} v_{rji}$.

come from a volume behavior law. The limit case of viscoplastic friction when $p = 0$ can be the Tresca friction law or can become the Coulomb friction law when α depends on the normal force. Its graph (F_t, v_t) is the same as for the Coulomb law.

3.3. *Approximation of the contact surface*

We denote by $P_1^{(k)}$ the position of the point, predicted at time t_1 by the velocity field for the approximation k, by $Q_1^{(k)}$ the projection of the point $P_1^{(k)}$ on the contact area with respect to the normal $\mathbf{n}_{21}^{(k)}$ to the reference solid (Fig. 8). When the analytical equations of the reference solid are known, as in the case of some forging tools, the normal can be analytically determined.

When the surfaces are discretized by differential surface elements, the predicted normal is a normal to the local differential surface element considered [1].

$P_1^{(k)}$ is calculated by

$$ {}^1x(k) = \mathbf{x}_0 + (\mathbf{v}_0 + {}^1\mathbf{v}_1^{(k)}) \frac{t_1 - t_0}{2}, \tag{35} $$

where $\mathbf{n}_{21}^{(k)}$ is the external normal to the reference solid at $P_1^{(k)}$.

The geometrical investigation phase, after a discretization of the boundary surface by local plans [27] leads to the prediction of the position of the point $P_1^{(k)}$ at time t_1 and the approximation k. When the impact point is close to several different surface elements, it is necessary to consider all the constraints coming from these possible contact areas.

The strategy of discretization seems to be better when the shapes are complex, mainly when all the considered solids are deformable. However is is possible to consider the discretization by other elements than plans.

4. SPACE–TIME DISCRETIZATION

Velocity formulation

According to the general formulation (19), we introduce the interpolation formulae

$$ \mathbf{v} = \mathbf{N}(\mathbf{x}, t)\, \dot{\mathbf{q}} \quad \text{and} \quad \mathbf{v}^* = \mathbf{N}^*(\mathbf{x}, t)\, \dot{\mathbf{q}}^*. \tag{36} $$

Here we also take the distribution of virtual parameters $\dot{\mathbf{q}}^*$ which depends only on the nodal parameters determined for $t = h$:

$$ \mathbf{N}^*(\mathbf{x}, t) = \left[\mathbf{0}; \mathbf{N}_{\alpha h}\left(\mathbf{x}, \delta\left(\frac{t}{h} - \alpha \right) \right) \right]. \tag{37} $$

We should here recall that the vectors $\dot{\mathbf{q}}$, $\dot{\mathbf{q}}^*$, $\dot{\mathbf{f}}$ are composed of two subvectors. The first one is defined for $t = 0$, the second one for $t = h$:

$$ \mathbf{q} = \begin{Bmatrix} \mathbf{q}|_{t=0} \\ \mathbf{q}|_{t=h} \end{Bmatrix}. \tag{38} $$

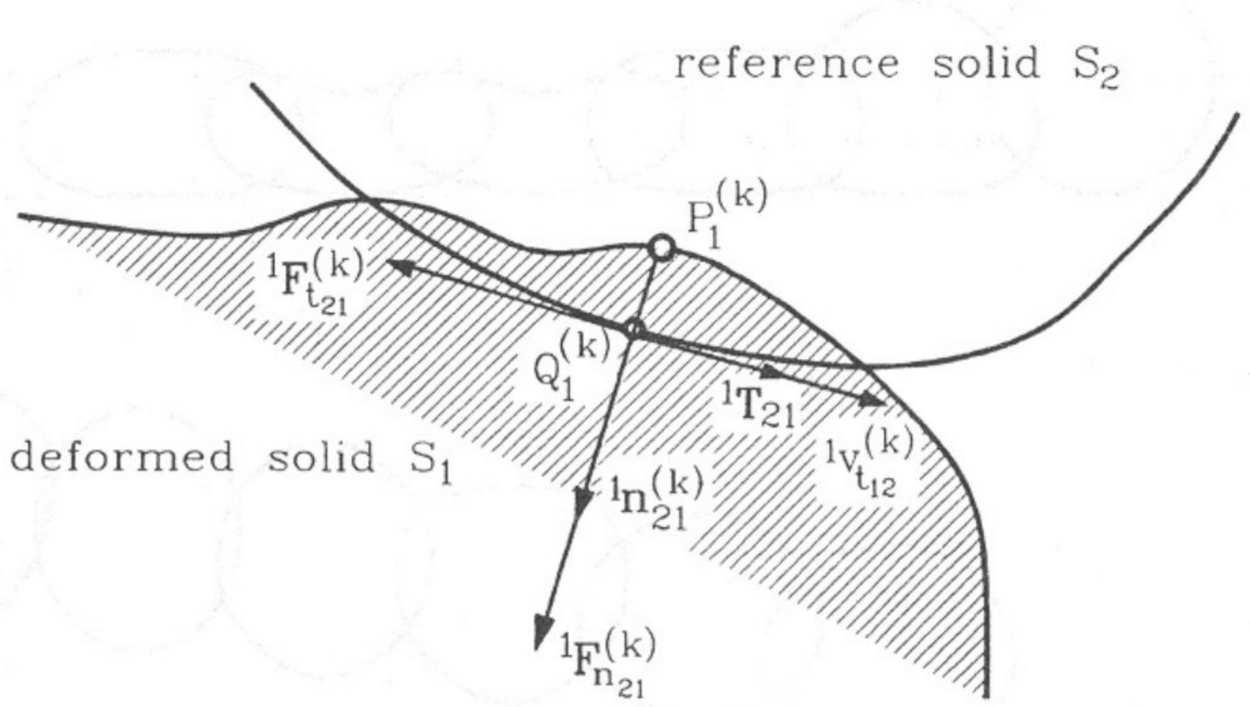

Fig. 8. Estimation of the unilateral contact force and friction force.

Finally we have:

$$\left\{\int_\Omega \left[(\mathscr{D}\mathbf{N}^*)^{\mathrm{T}}\mathbf{E}\mathscr{D}\int_0^t \mathbf{N}\,\mathrm{d}t\right]\mathrm{d}\Omega + \int_\Omega (\mathbf{N}^*)^{\mathrm{T}}\rho\frac{\partial \mathbf{N}}{\partial t}\,\mathrm{d}\Omega\right\}\dot{\mathbf{q}} + \int_\Omega (\mathscr{D}\mathbf{N}^*)^{\mathrm{T}}\mathbf{E}\epsilon_0\,\mathrm{d}\Omega = \int_\Omega (\mathbf{N}^*)^{\mathrm{T}}\mathbf{f}\,\mathrm{d}\Omega. \tag{39}$$

Since $\mathbf{N}^{*\mathrm{T}}$ is defined as the product of the Dirac distribution (37) by a space–time interpolation function, the integration over the space–time domain Ω is reduced to only the integration in space. However, shape matrices must be determined in particular moments. Then eqn (39) has a simple form:

$$(\mathbf{K}+\mathbf{M})\,\dot{\mathbf{q}} = \mathbf{F} - \mathbf{e}, \tag{40}$$

where

$$\mathbf{K} = \iint_{V_{\alpha h}} (\mathscr{D}\mathbf{N}_{\alpha h}(\mathbf{x}))^{\mathrm{T}}\mathbf{E}\mathscr{D}\mathbf{N}(\mathbf{x}, \alpha h/2)\,\mathrm{d}V\cdot\alpha h \tag{41}$$

$$\mathbf{M} = \iint_{V_{\alpha h}} \mathbf{N}_{\alpha h}^{\mathrm{T}}(\mathbf{x})\rho\frac{\partial \mathbf{N}(\mathbf{x}, \alpha h)}{\partial t}\,\mathrm{d}V \tag{42}$$

$$\mathbf{e} = \iint (\mathscr{D}\mathbf{N}_{\alpha h}(\mathbf{x}))^{\mathrm{T}}\mathbf{E}\epsilon_0\,\mathrm{d}V \tag{43}$$

$$\mathbf{F} = \iint_{V_{\alpha h}} \mathbf{N}_{\alpha h}^{\mathrm{T}}(\mathbf{x})\mathbf{f}(\mathbf{x})\,\mathrm{d}V. \tag{44}$$

Matrices **K** and **M** are the stiffness and mass matrices, respectively, the vector **e** is the vector of initial (in a given time interval) forces and **F** is the external load vector.

Large rotations

Let us denote by $d^{t_0}\mathbf{x}$ the vector determined in t_0. The vector $\mathrm{d}^t\mathbf{x}$ in time t is given as a result of tangential transformation

$$\mathrm{d}^t\mathbf{x} = {}^t_{t_0}\mathbf{F}\,\mathrm{d}^{t_0}\mathbf{x}. \tag{45}$$

Differentiation of eqn (45) with respect to t results in

$$\frac{\mathrm{d}^t\mathbf{x}}{\mathrm{d}t} = ({}^t\mathbf{W} + {}^t\mathbf{D})\,\mathrm{d}^t\mathbf{x} \tag{46}$$

where the term ${}^t\mathbf{W}^t\,\mathrm{d}\mathbf{x}$ is related to the rigid body motion

$${}^t\mathbf{W} = \tfrac{1}{2}(\mathrm{grad}\,\mathbf{v} - \mathrm{grad}^{\mathrm{T}}\mathbf{v}) \tag{47}$$

and the term ${}^t\mathbf{D}^t\,\mathrm{d}\mathbf{x}$ is related to the pure deformation

$${}^t\mathbf{D} = \tfrac{1}{2}(\mathrm{grad}\,v + \mathrm{grad}^{\mathrm{T}}\mathbf{v}). \tag{48}$$

After the decomposition

$${}^t_{t_0}\mathbf{F} = {}^t_{t_0}\mathbf{R}\,{}^t_{t_0}\mathbf{Y}, \tag{49}$$

the relation between the ${}^t_{t_0}\mathbf{R}$ and ${}^t\mathbf{W}$ can be determined as follows:

$$\frac{\mathrm{d}^t_{t_0}\mathbf{R}}{\mathrm{d}t}({}^t_{t_0}\mathbf{R})^{-1} - {}^t\mathbf{W} = \mathbf{0}. \tag{50}$$

The integration of eqn (50) results in the matrix of rotation in the interval $[t_0, t]$

$${}^t_{t_0}\mathbf{R}^{-1} = \mathbf{I}\,\mathrm{e}^{-{}^t\mathbf{W}(t-t_0)}, \tag{51}$$

which can be developed in series with two terms

$${}^t_{t_0}\mathbf{R}^{-1} = \mathbf{I} - (t-t_0){}^t\mathbf{W} + \frac{(t-t_0)^2}{2}{}^t\mathbf{W}^2. \tag{52}$$

The constitute relation for the hypoelastic material is described by

$$\frac{\mathrm{d}_J\boldsymbol{\sigma}}{\mathrm{d}t} = \mathbf{E}\mathbf{D}. \tag{53}$$

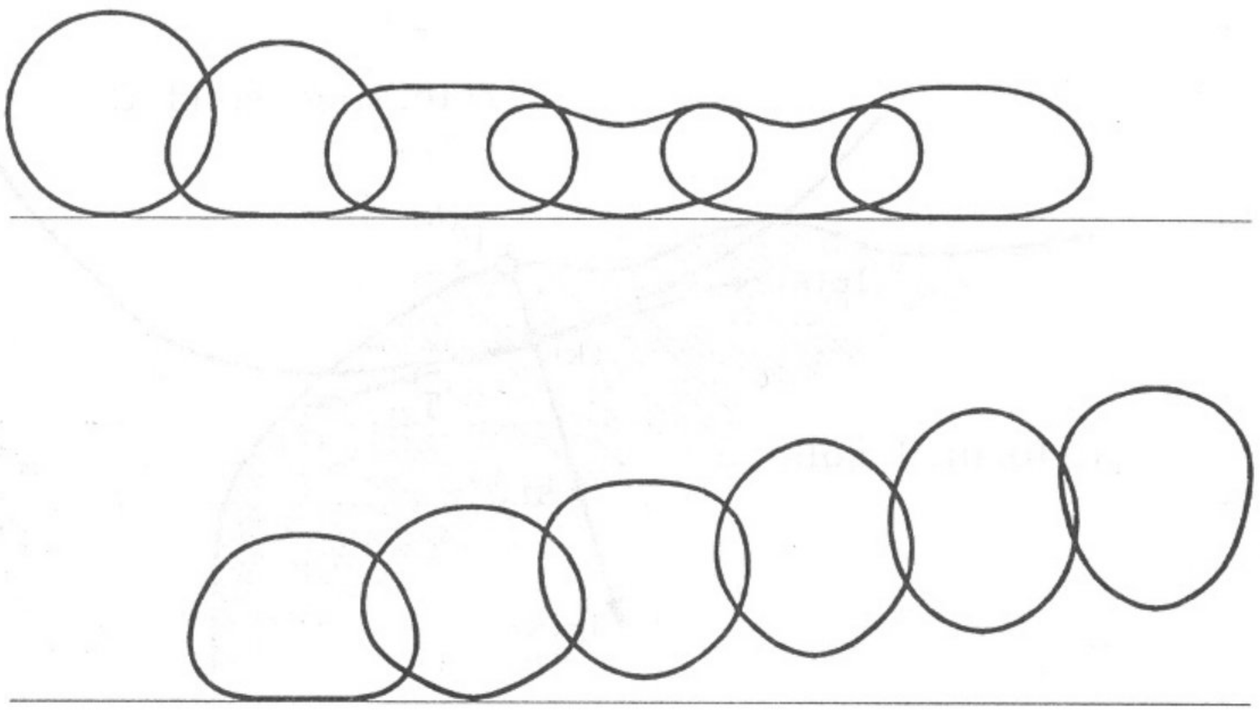

Fig. 9. Deformed ring in successive moments.

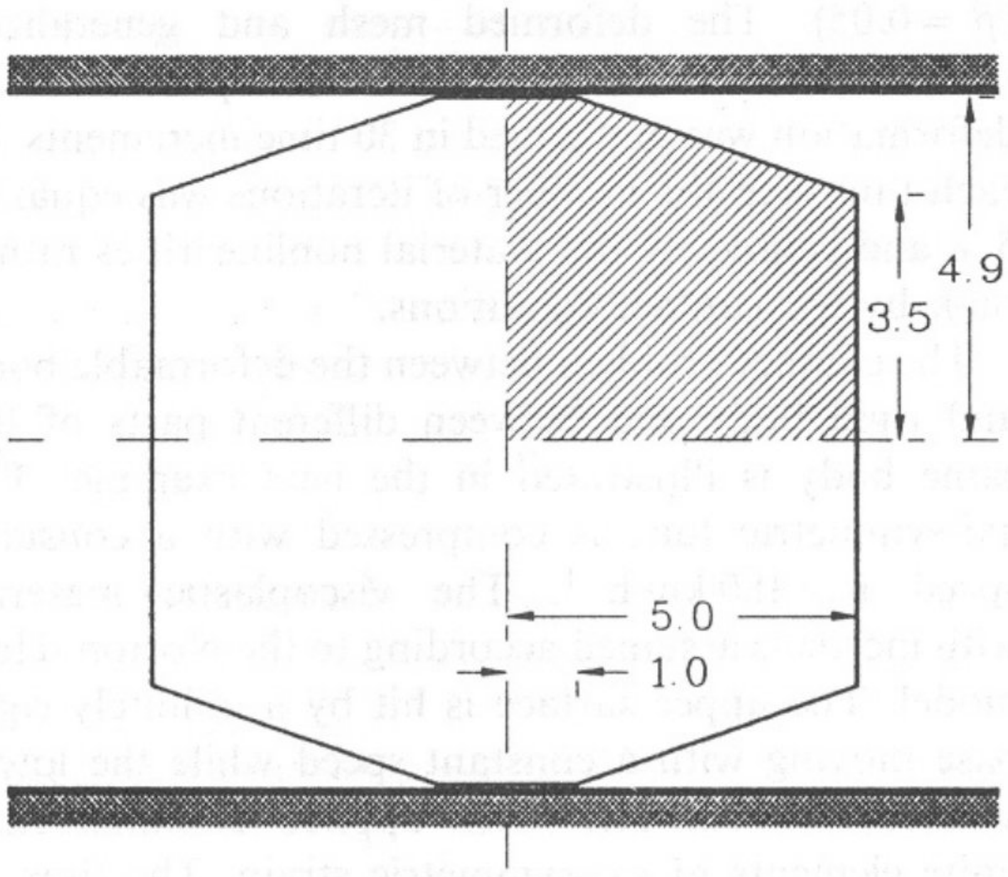

Fig. 10. The scheme of the compressed domain.

$d_J\boldsymbol{\sigma}/dt$ is the time derivative in corotational coordinate system and $\mathbf{D}$ is the rotation rate tensor. The deformation tensor in time t is described as

$$\boldsymbol{\sigma} = \boldsymbol{\sigma}_0 + \int_{t_0}^{t} \mathbf{ED}\, dt. \tag{54}$$

After the space–time discretization of the velocity vector (here linear distribution is assumed), in the base related to the configuration t_i,

$$\boldsymbol{\sigma} = ({}^{t}_{t_0}\mathbf{R})^{-1}\left(\boldsymbol{\sigma}_0 + (1-\alpha^2)\frac{h}{2}\right)\mathbf{ED}_0[({}^{t}_{t_0}\mathbf{R})^{-1}]^{\mathrm{T}}$$

$$+\alpha^2\frac{h}{2}\mathbf{ED}, \tag{55}$$

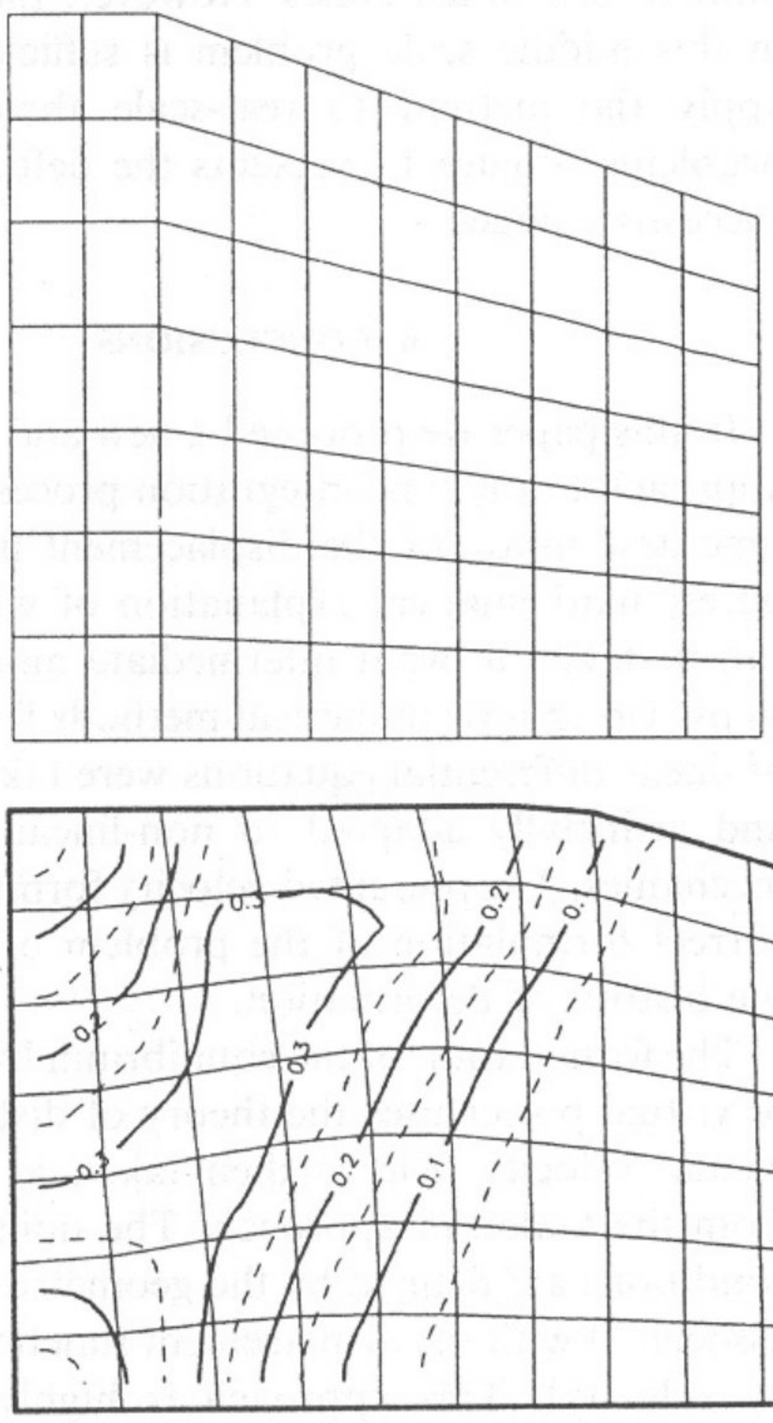

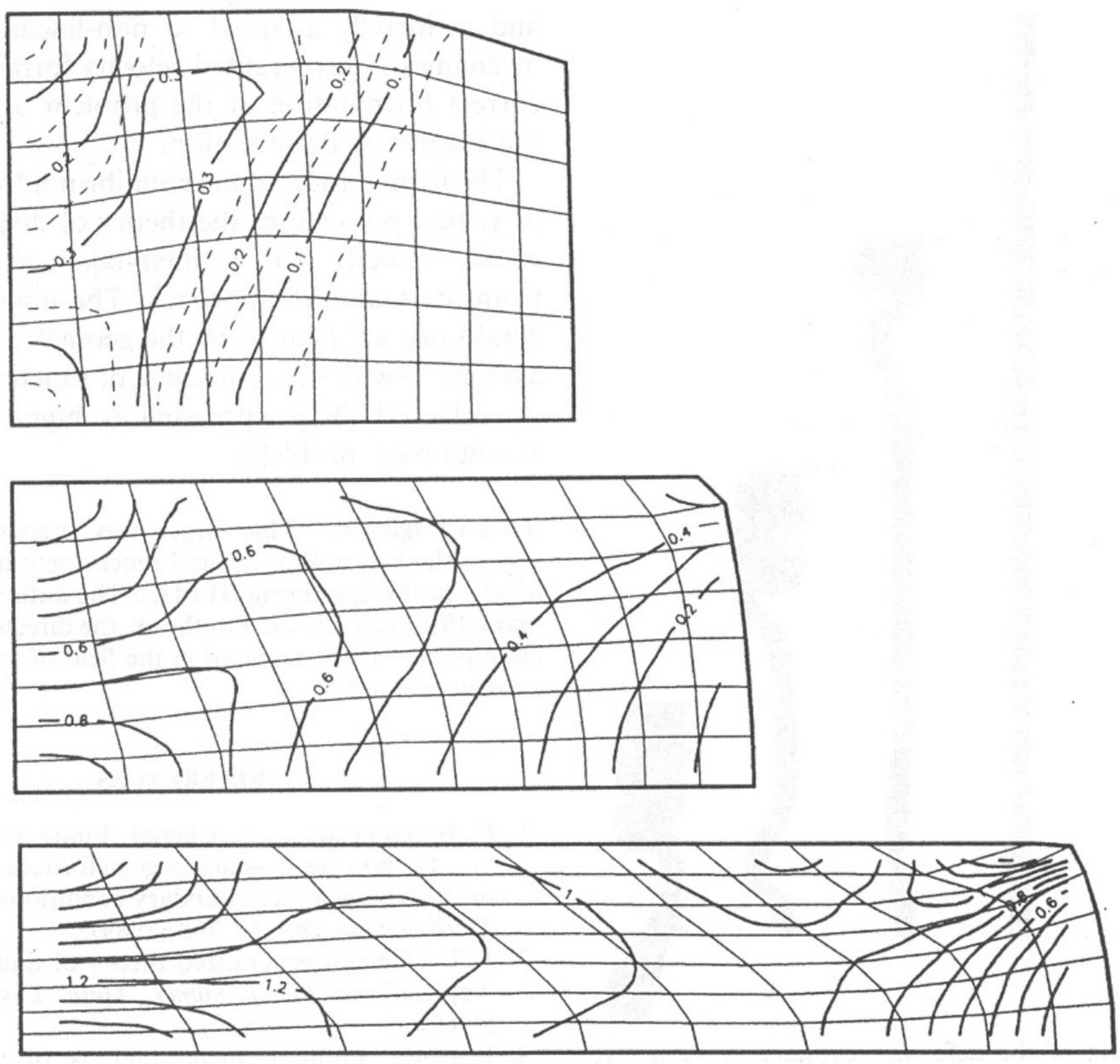

Fig. 11. Deformed mesh and generalized strain in the 10 steps (for $t = 0, 10, 20, 30$).

where $\alpha = (t_i - t_0)/h$, $h = t_1 - t_0$. The deformation determined by eqn (55) can be introduced to the equation of virtual work.

5. EXAMPLES

The presented method is efficient both for the time integration and the multi-contact analysis. Several simple tests proved the accuracy and efficiency of the approach. Here we will present only few examples to show the variety of problems that can be simply treated.

The first example concerns the elastic ring, which falls down on the rigid base. Material data and procedure parameters: $E = 0.004$, $A = 4.0$, $I = 0.333$, $\rho = 1.0$, $K = 1.2$, $\nu = 0.1$, $\Delta t = 25$, $v = 0.0015$. The half of the ring was discretized by 32 spatial elements. Successive forms of the ring are depicted in Fig. 9. The contact conditions were fulfilled in two to three iterations in every time step.

The next example which proves the efficiency of the velocity formulation is taken from Ref. [1]. A quarter of the eight-angular domain (Fig. 10) is compressed with the constant velocity $v = 0.1$. The material (Norton–Hoff model [29]) was assumed viscoplastic, according to the relations enclosed in that paper. The material constants were as follows: $m = 0.1$, $K = 1$, $\rho = 0.0$. Time step $\Delta t = 1$, velocity $v = 0.1$. On the upper surface the friction proportional to the tangential velocity v_t was applied: $T = -\beta |v_t|^{m-1} v_t$ ($\beta = 0.05$). The deformed mesh and generalized strain is depicted in Fig. 11. The whole process of the deformation was performed in 30 time increments. In each time step the number of iterations was equal to 5–8 and caused by the material nonlinearities rather than by the contact conditions.

The contact problem between the deformable body and rigid body and between different parts of the same body is illustrated in the next example. The axi-symmetric tube is compressed with a constant speed $v = 180\,\mathrm{km\,h^{-1}}$. The viscoplastic material with inertia is assumed according to the Norton–Hoff model. The upper surface is hit by a infinitely rigid base moving with a constant speed while the lower surface is fixed. The mesh applied contains 1250 finite elements of axi-symmetric strain. The time of calculation increases considerably with the increase in number of contact zones. However, the convergence in this middle scale problem is sufficiently good to apply the method to real-scale three-dimensional problems. Figure 12 presents the deformed mesh in successive stages.

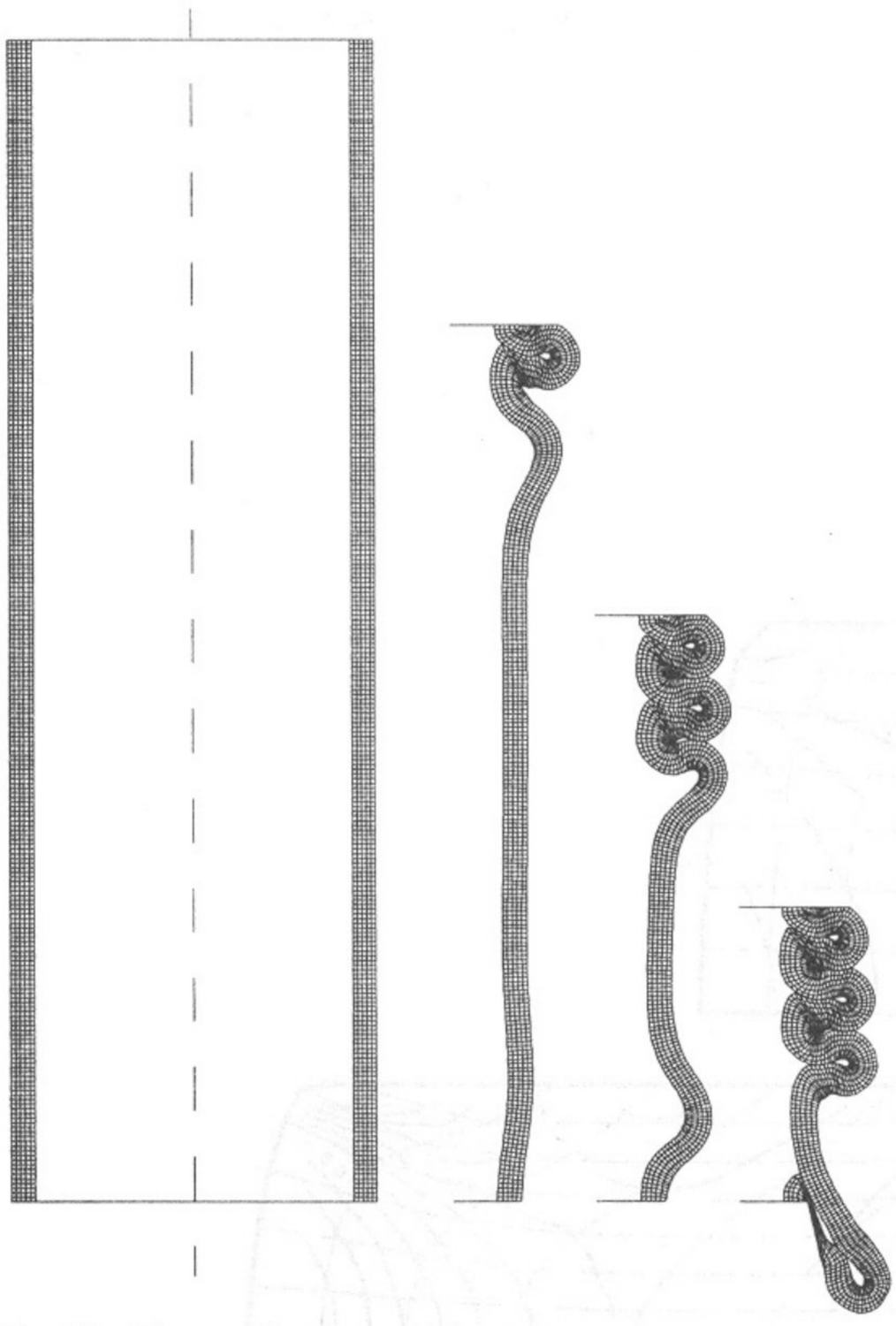

Fig. 12. The mesh of the deformed cylinder in successive steps.

6. CONCLUSIONS

In this paper we proposed a new and more efficient approach to the time integration process. The space–time description of the displacement fields gives the purely mathematical explanation of what quantities can be taken in what intermediate moments in time steps. Up to now numerical methods for the solution of linear differential equations were taken in practice and artificially adapted to non-linear equations of mechanics. The presented velocity formulation allows correct formulation of the problem of evolution by the history of deformation.

The formulation of the equilibrium by the principle of virtual power uses the theory of distribution. The virtual velocity field is then taken a different way from the Galerkin approach. The unilateral contact conditions are defined by the geometrical constraints associated with the displacement functions (described by velocity). This approach is highly efficient for evolutionary problems.

Acknowledgement—This paper was prepared during the stay of the first author at the French Institute of Advanced Mechanical Engineering (IFMA). The author would like to thank Professor Claude Bonthoux, the director of IFMA for his support for the research in the field of space–time finite element method.

REFERENCES

1. C. Bohatier and J.-L. Chenot, Finite element formulation for non-steady-state large deformations with sliding or evolving contact boundary conditions. *Int. J. numer. Meth. Engng* **28,** 753–768 (1989).
2. J. T. Oden, A generalized theory of finite elements, II. Applications. *Int. J. numer. Meth. Engng* **1,** 247–259 (1969).
3. I. Fried, Finite element analysis of time-dependent phenomena. *AIAA J.* **7,** 1170–1173 (1989).

4. J. H. Argyris and A. S. L. Chan, Application of the finite elements in space and time. *Ing. Archiv* **41,** 235–257 (1972).
5. J. H. Argyris and D. W. Scharpf, Finite elements in space and time. *Nucl. Engng Des.* **10,** 456–469 (1969).
6. J. H. Argyris and D. W. Scharpf, Finite elements in time and space. *Aeron. J. R. aeron. Soc.* **73,** 1041–1044 (1969).
7. Z. B. Kuang and S. N. Atluri, Temperature field due to a moving heat source. *J. appl. Mech. Trans. ASME* **52,** 274–280 (1985).
8. Z. Kaczkowski, The method of finite space–time elements in dynamics of structures. *J. tech. Phys.* **16**(1), 69–84 (1975).
9. Z. Kaczkowski, General formulation of the stiffness matrix for the space–time finite elements. *Arch. Inż. Ląd.* **25**(3), 351–357 (1979).
10. Z. Kaczkowski and J. Langer, Synthesis of the space–time finite element method. *Arch. Inż. Ląd* **26**(1), 11–17 (1980).
11. C. I. Bajer, Notes on the stability of non-rectangular space–time finite elements. *Int. J. numer. Meth. Engng* **24,** 1721–1739 (1987).
12. Z. Kacprzyk and T. Lewiński, Comparison of some numerical integration methods for the equations of motion of systems with a finite number of degrees of freedom. *Engng Trans.* **31**(2), 213–240 (1983).
13. W. Witkowski, Dynamic analysis of hoist cable using triangular space–time elements. *Engng Trans.* **34**(4), 445–456 (1986).
14. C.I. Bajer, Triangular and tetrahedral space-time finite elements in vibration analysis. *Int. J. numer. Meth. Engng* **23,** 2031–3048 (1986).
15. C. I. Bajer, Adapative mesh in dynamic problem by the space–time approach. *Comput. Struct.* **33**(2), 319–325 (1989).
16. C. Bajer, R. Bogacz and C. Bonthoux, Adaptive space–time elements in the dynamic elastic–viscoplastic problem. *Comput. Struct.* **39,** 415–423 (1991).
17. C. Bohatier, A large deformation formulation and solution with space–time finite elements. *Arch. Mech.* **44,** 31–41 (1992).
18. A. Podhorecki, The viscoelastic space-time element. *Comput. Struct.* **23,** 535–544 (1986).
19. C. I. Bajer and C. G. Bonthoux, State-of-the-art in true space–time finite element method. *Shock Vibr. Dig.* **20,** 3–11 (1988).
20. C. I. Bajer and C. G. Bonthoux, State-of-the-art in the space-time element method. *Shock Vibr. Dig.* **23**(5), 3–9 (1991).
21. C. Bajer and A. Podhorecki, Space–time element method in structural dynamics. *Arch. Mech.* **41,** 863–889 (1989).
22. N. Kikuchi and J. T. Oden, *Contact Problems in Elasticity: a Study of Variational Inequalitites and Finite Element Method.* SIAM (1988).
23. A. B. Richelsen, Friction modelling in a finite strain viscoplastic analysis of a rolling process. In *Euromech* 273, *Unilateral Contact and Dry Friction*, pp. 121–124. La Grande Motte, France (1990).
24. P. Alart, A mixed formulation for frictional contact problems prone to Newton-like solution methods. *Comput. Meth. appl. mech. Engng* **92**(3), 353–375 (1991).
25. A. Cournier and J. H. Heegaard, An augmented Lagrangian method for large slip contact problems. In *Euromech* 273, *Unilateral Contact and Dry Friction*, pp. 69–72. La Grande Motte, France (1990).
26. J. J. Moreau, P. D. Panagiotopoulos and G. Strang, *Topics in Nonsmooth Mechanics*. Birkhäuser (1988).
27. M. Jean, Implementation of unilateral contact and dry friction in computer codes dealing with large deformations problems. *J. theor. appl. Mech.* **7,** special issue, suplement no. 1 (1988).
28. J. J. Moreau, *Unilateral Contact and Dry Friction in Finite Freedom Dynamics*, pp. 11–82. Number 302 in CISM Courses and Lectures, Springer, Berlin (1988).
29. N. J. Hoff, Approximate analysis of structures in the presence of moderately large creep deformation. *Q. appl. Math.* **12**(1), 49 (1954).